JOURNAL OF APPLIED ELECTROCHEMISTRY 20 (1990) 60–68

HBr electrolysis in the Ispra Mark 13A flue gas desulphurization process: electrolysis in a DEM cell

D. VAN VELZEN, H. LANGENKAMP, A. MORYOUSSEF

Commission of the European Communities, Joint Research Centre – Ispra Establishment, 21020 Ispra (Va), Italy

P. MILLINGTON

The Electricity Council Research Centre, Capenhurst, Chester CH1 6ES, UK

Received 13 January 1989; revised 17 April 1989

The potential application of a DEM cell for the electrolysis of hydrogen bromide in the Ispra Mark 13A process for flue gas desulphurization has been tested in a number of laboratory experiments and in long-duration tests in a bench-scale plant of the process. Satisfactory electrode materials have been found, i.e. Hastelloy C 276 for the cathode and a RuO_2 coating on titanium for the anode. Both electrode materials showed a good stability during a 1500 hours experiment. Cell voltage/current density relationships have been determined during bench-scale plant operation. A typical value is 1.5 V at a current density of 2.5 kA m^{-2}. It has been shown that in an undivided cell a cathodic back reaction occurs which causes a decrease of the current efficiency. Under normal operation conditions current efficiencies of about 90% are obtained.

A simplified flow model for the DEM cell was developed which is useful in understanding the phenomena which occur during scale-up of the cell. An industrial size installation for the production of 170 kg h^{-1} of bromine at a current density of 2 kA m^{-2} was constructed and has been in operation since August 1989.

Nomenclature

a_x	thermodynamic activity of the constituent x (mol cm^{-3})
C	bromine concentration (mol l^{-1})
e_z	local current efficiency
e_{ov}	overall cell efficiency
E_a^0	anodic standard potential (V)
E_c^0	cathodic standard potential (V)
E_a^e	equilibrium anode potential (V)
E_e^e	equilibrium cathode potential (V)
F	Faraday number (C mol^{-1})
g_a	anodic overpotential (V)
g_c	cathodic overpotential (V)
G	electrolyte flow rate (l h^{-1})
i	current density (A m^{-2})
K_c	cathodic back reaction rate factor (l mol^{-1})
L	cell width (m)
n	number of electrons involved ($n = 2$)
R	gas constant (J K^{-1} mol^{-1})
R_{cell}	cell resistance (ohm m^2)
R_c	circuit resistance (ohm m^2)
w_b	local cathodic back reaction rate (mol m^{-2} h^{-1})
w_{th}	local theoretical reaction rate (mol m^{-2} h^{-1})
W_{th}	overall theoretical reaction rate (mol h^{-1})
T	temperature (K)
Z	cell length (m)

1. Introduction

1.1. *Background*

Flue gas desulphurization (FGD) is the process which removes pollutant sulphur dioxide from flue gases produced by the combustion of fossil fuels in power stations and other large scale combustion installations. FGD is applied on a very large industrial scale in the Federal Republic of Germany, the United States and Japan. The most common method employs wet scrubbing with lime or limestone, which produces gypsum or calcium sulphite slurries [1, 2]. This method has some intrinsic drawbacks: large quantities of wet slurries have to be handled, considerable amounts of waste water are produced, and the disposal of large quantities of gypsum may cause problems.

Regenerable FGD processes may therefore offer certain advantages. Several systems are already installed or under development [3, 4], but important investigations are still being carried out in this area [5]. The Ispra Mark 13A process for flue gas desulphurization is a new wet scrubbing regenerative FGD process. It has been invented at the Joint Research Centre of Ispra (Italy) of the European Community [6]. This process produces two valuable chemicals, sulphuric acid and hydrogen, and is based on the two following

0021-891X/90 $03.00 + .12 © 1990 Chapman and Hall Ltd.

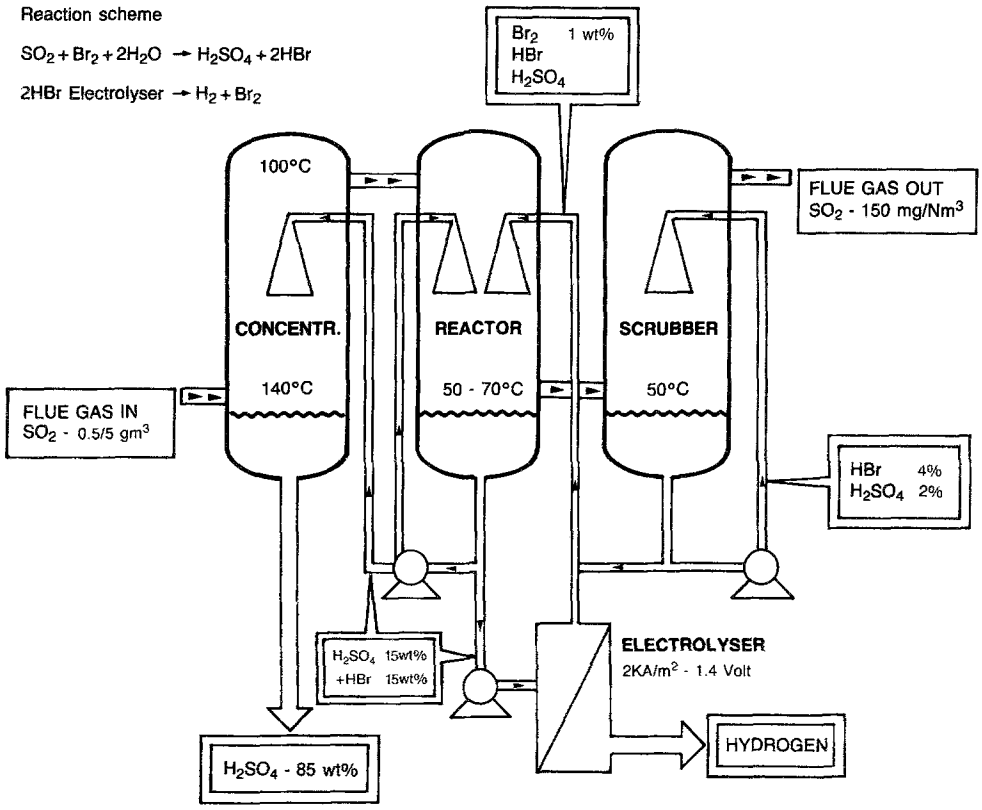

Fig. 1. Block scheme of the Ispra Mark 13A process for flue gas desulphurization.

chemical reactions:

$$SO_2 + Br_2 + 2H_2O \longrightarrow H_2SO_4 + 2\,HBr \qquad (1)$$

$$2HBr \longrightarrow H_2 + Br_2 \quad \text{(electrolysis)} \qquad (2)$$

A block scheme of the process is presented in Fig. 1. The reactive agent is a dilute aqueous solution of about 15 wt% H_2SO_4/15 wt% HBr containing a small amount of bromine (< 1 wt%). The SO_2-containing flue gases are brought in contact with this solution in the reactor. Sulphur dioxide is absorbed in the solution and reacts immediately in the liquid phase according to Reaction 1. In this reaction, the bromine conversion is 100%, a bromine free washing liquid is produced and the reaction products, HBr and H_2SO_4, stay dissolved in solution.

The bromine required for the removal of SO_2 is produced by electrolysis of hydrobromic acid (reaction (2)). Bromine acts as an oxidizing agent, converting SO_2 into sulphuric acid. Reactions 1 and 2 are carried out at 55–60° C. Sulphuric acid is produced in the reactor liquid, from which it has to be concentrated and separated. This separation is carried out by evaporation, making use of the sensible heat of the incoming flue gas (150–200° C). A side stream of the reactor liquid is fed to the concentrator where it flows counter-current to part of the incoming flue gas. In this operation, all the HBr and a large part of the water from the reactor are evaporated and an 80–85 wt% sulphuric acid is produced. In industrial size versions of the process, this acid is further concentrated to 90–95 wt% in a separate final concentrator. A gas stream of about 300° C is used for this purpose. The bench-scale unit used in the present electrolytic experiments does not contain such a final concentrator. The desulphurized flue gas, leaving the reactor, still contains some reactor liquid droplets and HBr vapour. These contaminants are washed out with water in a final scrubber downstream of the reactor, and returned to the reactor liquid.

A pilot/demonstration plant of the Ispra Mark 13A process has been in operation since November 1988. This plant has a capacity of 32 000 $m^3\,h^{-1}$ of flue gas and is situated at the SARAS Refinery at Sarroch near Cagliari in Sardinia [7]. The sulphur dioxide content of the flue gas is 4.5 $g\,m^{-3}$ and the amount of treated flue gas is equivalent to that produced by a power station of capacity 13 MWe.

The most innovative part of the Ispra Mark 13A process is the HBr electrolysis in a mixed HBr/H_2SO_4 electrolyte. The production of the active reagent (Br_2) by electrolysis avoids the addition of chemicals to the process, i.e. consumption, storage facilities, etc. However, this advantage is counterbalanced by an increase in the power consumption of the process. In the Sarroch pilot plant the bromine production rate needed for a 90% desulphurization is 320 $kg\,h^{-1}$ (2 $kmol\,h^{-1}$). This requires an electrolysis current of about 110 kA. The individual cell voltage is between 1.3 and 1.4 V, so that the power consumption for electrolysis is approximately 150 kWe, i.e. 1.2% of the plant output. Here, it must be taken into account that the calorific value of the hydrogen produced in the electrolysis (50 $Nm^3\,h^{-1}$) amounts to 170 kW, which partly compensates the electrolysis power consumption.

The energy content of the incoming flue gases is largely sufficient for the concentration of the sulphuric

acid, and a part of the excess energy can be used for the reheating of the treated flue gases before being passed to the chimney. The economic outlook of the process is promising.

1.2. *The electrolysis*

The purpose of this paper is to report on the hydrobromic acid electrolysis in the experimental conditions of the Ispra Mark 13A FGD process, i.e. in a mixed HBr/H_2SO_4 electrolyte, at temperatures around 60° C and generally in the presence of an excess of SO_2.

Hydrobromic acid electrolysis has mainly been studied in concentrated solutions (47.5 wt%) and with graphite electrodes. Fiebelmann and Schütz [8] carried out this electrolysis in concentrated solutions at graphite electrodes over a temperature range of 80–200° C. At 100° C, they found a value of 0.8 V for the cell voltage at a current density of $2\,kA\,m^{-2}$. Anode life tests were carried out at 100° C and at $1\,kA\,m^{-2}$ which showed an excellent stability of the graphite electrodes over a long period (14 000 h).

Fees *et al.* [9] reported results on the influence of noble metal catalysts on the electrochemical decomposition of concentrated HBr at graphite electrodes, and proved that platinum deposition considerably reduced the hydrogen evolution overvoltage at the cathode. They also studied the effect on cell voltage of temperature, inter-electrode gap and bromine concentration. The use of metallic electrodes for the electrolysis of hydrobromic acid has not been reported and no recent data are available for the electrolysis of HBr in dilute $HBr–H_2SO_4$ mixtures.

The electrolytic decomposition of hydrogen bromide proceeds in two steps. The first is the cathodic reaction:

$$2H^+ + 2e \longrightarrow H_2 \qquad (3)$$

The equilibrium potential E_e^c is expressed by the Nernst equation:

$$E_e^c = E_c^0 + RT/nF \ln (a_{(H+)}^2/a_{H_2}) \qquad (4)$$

The second step is the anodic reaction:

$$2Br^- \longrightarrow Br_2 + 2e \qquad (5)$$

where the standard potential $E_a^0 = 1.07$ V versus NHE and the equilibrium potential is expressed by:

$$E_e^a = E_a^0 + RT/nF \ln (a_{Br_2}/a_{(Br^-)}^2) \qquad (6)$$

The total cell voltage can then be expressed by:

$$V = E_e^c - E_e^a - g_a - g_c - IR_{cell} - IR_c \qquad (7)$$

where g_a and g_c are the absolute values of the anode and the cathode overpotentials.

The main advantages of the use of bromine as an oxidant for sulphur dioxide are related to the low standard potential of the Br^-/Br_2 redox couple compared to that for the Cl^-/Cl_2 system (1.066 V against 1.36 V versus NHE): the energy consumption is low and oxygen evolution does not compete with bromine formation at the anode at the low pH values applied in the process.

1.3. *The cathodic back reaction*

During the electrolysis of hydrobromic acid hydrogen gas is evolved at the cathode, whereas at the anode the production of bromine takes place. The latter forms a homogeneous solution with the electrolyte. The applied DEM cell is an undivided cell, i.e. it operates without any separation of the anodic and cathodic compartments. It follows that in the cell there is an upward co-current flow of hydrogen gas and bromine-containing electrolyte. In practice, this forms a homogeneous, upward flowing two-phase mixture. As an example, the normal flow rate of electrolyte through the cell is about $200\,l\,h^{-1}$, which gives rise to an upward linear velocity of $4.5\,cm\,s^{-1}$. At a current density of $2\,kA\,m^{-2}$, the hydrogen formation rate is approximately $40\,l\,h^{-1}$. This means that a considerable part of the cell volume is occupied by small hydrogen bubbles. The upward velocity of the hydrogen bubbles is larger than the electrolyte flow, which causes a thorough mixing of the fluid phase during its passage through the cell. It is therefore inevitable that some of the bromine, formed at the anode, reaches the cathode surface where the following reaction then occurs:

$$2e + Br_2 \longrightarrow 2Br^- \qquad (8)$$

Reaction (8) is called the 'cathodic back reaction'. This reaction causes losses in the current efficiency of the electrolytic process.

In this present paper the current efficiency is one of the main subjects being studied. It is obvious that the bromine content of the electrolyte at the cell inlet has a strong influence on the efficiency, but the current density, the electrolyte flow rate and the cell dimensions also play an important role. The development of a simple cell reaction model proves to be helpful in understanding the observed phenomena.

2. Experimental method

2.1. *The DEM cell*

The electrochemical cell used for the laboratory tests was developed by the Electricity Council Research Centre (Capenhurst, Chester, England) and is manufactured under license by Electrocatalytic Ltd. It is known as the 'Dished Electrode Membrane' cell (DEM cell). All experiments were performed with a bench scale cell having a single electrode area of $500\,cm^2$. The cell is shown in Fig. 2. It is an undivided monopolar electrolyser fitted with metallic electrodes which consist of a dished cathode (Hastelloy C) and a flat coated anode. The interelectrode gap is small, 4–5 mm, thereby minimizing the internal resistance of the cell, and hence the cell voltage. The dishing of the electrode allows a comparatively thick cell frame to be used, which accomodates large electrolyte ports for connections to external manifolds. High electrolyte flow rates can easily be accomodated which is essential for high mass transport conditions. The use of heavy gauge aluminium current distribution plates in the

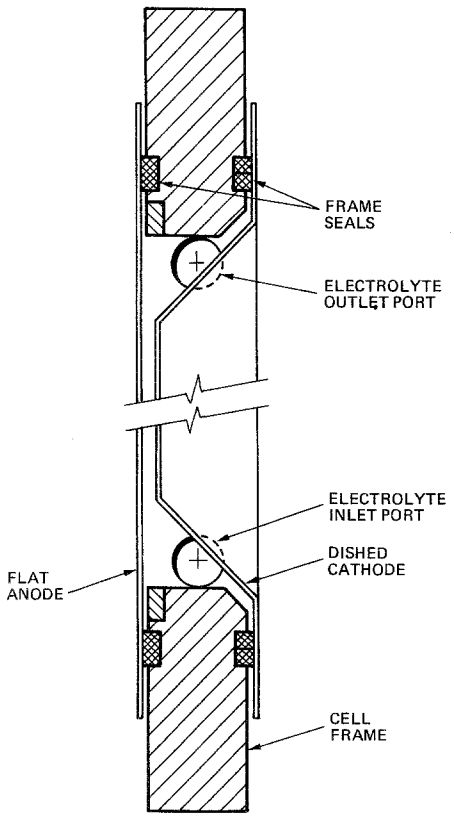

Fig. 2. Cross-section of an undivided DEM cell.

DEM cell provides a good current distribution across the face of the electrode.

Attention has been focussed on the electrochemical parameters (minimization of the cell voltage and increase in efficiency) in order to optimize energy cost and investment. The effect of bromine concentration, electrolyte flow rate, temperature, and noble metal deposition at the cathode have been examined. As the use of metallic electrodes is a novelty in the electrochemical decomposition of hydrobromic acid, a careful control of the corrosion rate of both electrodes has been carried out. It must be noted that the DEM cell has already found a number of industrial applications [10], but had never been tested for bromine production at such low pH.

The anode material must preferably show a low overpotential for Br_2 evolution and a high O_2 overpotential. A dimensionally stable anode (DSA) consisting of a mixed RuO_2/TiO_2 coating on a flat titanium sheet was chosen. This material is industrially used for chlorine electrolysis, where the chlorine overpotential is as low as 5 to 40 mV [11]. The oxygen overpotential on this electrode material has been determined by Scarpellino [12] and is approximately 200 mV. As far as the cathode is concerned, a low H_2 overpotential and a good resistance in the corrosive electrolyte are required. The selected cathode material was Hastelloy C 276. The main constituent of this alloy is Ni. The exchange current density for hydrogen evolution on nickel has been determined by Trasatti [13] and is equal to 10^{-4} A m^{-2}. From this data the hydrogen overpotential can be calculated. This is approximately 400 mV at room temperature and a current density of 1 kA m^{-2}.

During standby periods, an independent power supply has to be connected to the cell which is operated at a minimum current density of 25 A m^{-2} to prevent corrosion of both electrodes. The cathodic protection potential required to avoid corrosion at low pH is about 400 mV [14].

2.2. *Operation*

The electrolytic cell is only operated in combination with the bench scale unit of the flue gas desulphurization process. This prevents accumulation of bromine and maintains a constant composition of the electrolyte. The Ispra Mark 13A bench scale plant (Fig. 1) is able to treat a volume flow of about 10 m^3 h^{-1} flue gas which is produced by the combustion of heavy fuel oil (2.7 wt% S). Normally, the SO_2 content of the flue gas is 2000 ppm. There is the possibility of adding SO_2 from a gas bottle, so that higher concentrations can also be produced. The sulphur dioxide throughput is thus between 1 and 4 mol h^{-1}, requiring the production of the equivalent quantity of bromine. This corresponds to a current flow through the electrolyser of between 50 and 200 A and a current density in the range of 1 to 4 kA m^{-2}. The flow rate of electrolyte through the cell is varied between 150–300 kg h^{-1}, which is equivalent to a linear velocity of 3–7 cm s^{-1}. The reactor liquid temperature is in the range 45–60° C. The HBr and H_2SO_4 content of the electrolyte can both be varied from 10 to 20 wt%. The total quantity of electrolyte circulating is approximately 20 kg, which corresponds to a volume of 17.5 l.

2.3. *Cell voltage and cathodic efficiency measurements in normal operating conditions*

The desired current density is applied across the cell by means of a Hewlett Packard power supply 6553A (0–15 V; 0–200 A), and the quantity of sulphur dioxide entering the system is adjusted so that it is always stoichiometrically in excess of the amount of bromine formed anodically (200 ppm of SO_2 in the outlet). After stabilization, the hydrogen production is measured by means of a wet gasometer (Wilhem Ritter), and the stabilized cell voltage is read on the power supply. The cathodic current efficiency is calculated using Faraday's law.

2.4. *Anodic current efficiency measurements*

The measurements are carried out as follows: before the experiment is started, it is ascertained that the electrolyte is free of bromine (less than 0.02 wt%). Then, the flue gas supply system is put in by-pass so that no SO_2 can flow through the system. The current is then increased to the desired value and samples at the outlet of the electrolyser are taken every 5 min for a total of 20 to 25 min. The bromine content of the electrolyte is analysed by iodometric titration. In the meantime, the hydrogen production rate is followed.

When the experiment is terminated, the current is

decreased to a minimum, and samples are analysed at the inlet and outlet of the electrolyser after 5 and 10 minutes in order to make sure that the bromine formed during the experiment is homogeneously mixed in the electrolyte. The Br_2 production rate can be derived from the bromine content of the electrolyte (the mass of circulating electrolyte is known) and the efficiency calculated. A comparison between anodic and cathodic current efficiencies is then possible.

2.5. *Influence of inlet bromine concentration on the efficiency*

The steps of this experiment are essentially the same as for the anodic efficiency measurements. The main difference is that in the present case the duration of the experiment is prolonged to at least 40 min. In this way very low current efficiencies, down to 30 and 40%, are obtained and a thorough study of the cathodic back reaction can be carried out.

The hydrogen production rate is measured continuously and gives an indication of the overall cell efficiency. Thus, the decrease of the electrochemical efficiency as a consequence of the increasing bromine content of the electrolyte is determined. When the experiment is terminated, SO_2 is reintroduced into the system and the accumulated Br_2 is subsequently converted into HBr and H_2SO_4.

2.6. *Anode coating thickness measurements*

As the integrity of the anode coating is the key to the success of the bromine generator, two sets of data on anode life tests were collected: one set under accelerated life conditions in the laboratory, and the other by monitoring the anode used in the pilot plant.

The accelerated life tests were carried out in a large tank cell (51 capacity), which was sealed with the exception of a single outlet protected by a water cooled condenser. The cell accomodates ten test anodes. Each anode is in the form of a spade (1 cm^2 area) spot welded to a titanium rod. Both faces of the spade and the rod are coated. The electrodes are arranged on both sides of a large area (100 cm^2) nickel cathode. The gap between the working face of the spade and the cathode is similar to that (4–6 mm) in the pilot plant cell. The thickness of the coating is measured by X-ray fluorescence (Fischerscope X-Ray 1000, Fischer Instrumentation (GB) Ltd). The instrument requires calibration with known standards in order to measure absolute values for coating thickness. In the case of the accelerated life tests, no standards were available, so that only relative changes in thickness can be given. In contrast, samples of known coating thickness are available for the anode used in the pilot plant. Consequently, here the actual coating thicknesses could be measured.

3. Simple cell reaction model

In a monopolar electrolytic cell the theoretical production of bromine and hydrogen per units of electrode surface is given by Faraday's Law:

$$w_{th} = 3600\, i/nF \tag{9}$$

The total production for a cell is then given by:

$$W_{th} = w_{th} LZ \tag{10}$$

For the present cell dimensions, $L = Z = 0.224$ m, it follows that

at 1.0 kA m^{-2} (50 A): $W_{th} = 0.933$ mol h^{-1}
at 1.5 kA m^{-2} (75 A): $W_{th} = 1.400$ mol h^{-1}
at 2.0 kA m^{-2} (100 A): $W_{th} = 1.865$ mol h^{-1}

The local rate of the back reaction is expressed by:

$$w_b = w_{th}(1 - e_z) \tag{11}$$

where e_z is the local current efficiency. From the reasoning given earlier it is evident that the rate of the back reaction must be dependent on C, the bromine concentration in the electrolyte. This dependency is such that $e_z = 1$ when $C = 0$ and that $e = 0$ when C becomes large. The numerical value of e must remain between 0 and 1 for all current values of C.

It can be assumed, as a first approximation, that the back reaction is first order with respect to the bromine concentration, and also depends on the current density. The following rate equation is proposed:

$$w_b = w_{th} K_c C \tag{12}$$

In a vertical undivided DEM cell the radial mixing rate is high and the rate of axial mixing is low. In this case, the flow of electrolyte through the cell can be represented by a plug flow model with superimposed ideal mixing in the radial direction. This simple cell flow model assumes that there is no radial gradient in the bromine concentration and that no backmixing occurs. The development of the bromine concentration (C) as a function of cell length in the flow direction (Z) can now easily be calculated.

A mass balance over a small cell element dZ in the flow direction gives:

$$G\,dC = L(w_{th} - w_b)\,dZ \tag{13}$$

Combination of (12) and (13) and rearrangement yields:

$$(w_{th} L/G)\,dZ = dC/(1 - K_c C) \tag{14}$$

At $Z = 0$, $C = C_{in}$ and at $Z = Z$, $C = C_z$. Integration from $Z = 0$ to $Z = Z$ yields:

$$K_c w_{th} ZL/G = \ln(1 - K_c C_{in}) - \ln(1 - K_c C_z) \tag{15}$$

Once K_c is known the profile of the bromine concentration over the cell can be calculated. On the other hand, when in any experiment the current density, the bromine inlet and outlet concentration, and/or the current efficiency are known, the corresponding numerical value of K_c can be calculated.

Here it must be noted that by Equation 15 *local* bromine concentrations and thus *local* current efficiencies can be calculated. The *overall* cell efficiency

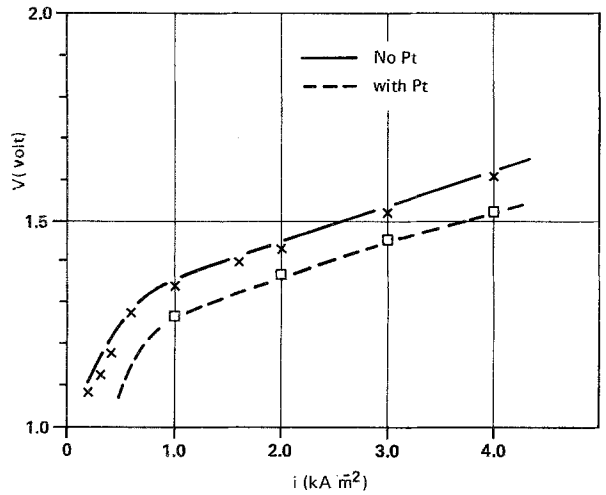

Fig. 3. Current/voltage curve at 50° C. Flow rate: 190 l h^{-1}; electrolyte composition: 15 wt% HBr–14 wt% H_2SO_4.

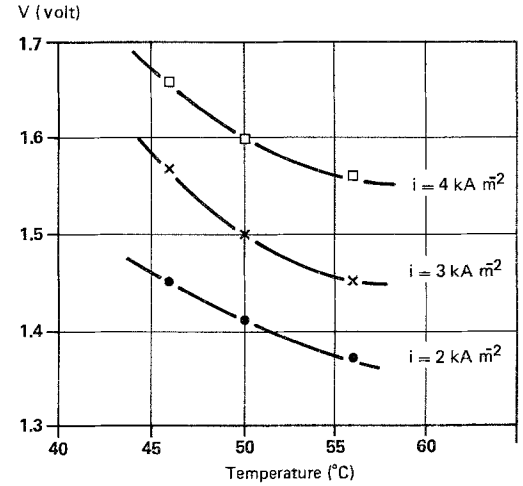

Fig. 4. The influence of temperature on cell voltage.

follows from a mass balance over the inlet and the outlet of the cell and is given by:

$$e_{ov} = G(C_z - C_{in})/W_{th} \quad (16)$$

4. Results and discussion

4.1. *Current–voltage characteristics*

The cathode material has a substantial influence on the exchange current density and hence the cathode overpotential. Noble metals (Pt, Pd, Rh. . .) are known to have a high exchange current density and, therefore, a low overvoltage for hydrogen evolution [9, 13]. For this reason, cell voltage measurements have been carried out with and without the addition of a platinum salt, $PtCl_4$, in the reactor liquid. The quantity of $PtCl_4$ added ensures that about 2.5 mg cm^{-2} of Pt is deposited at the cathode surface. The results were obtained under the following experimental conditions:

Temperature	50° C
Flow rate	190 l h^{-1}
Electrolyte composition	15 wt% HBr–14 wt% H_2SO_4

Figure 3 represents a plot of the cell voltage against current density, in the absence and in the presence respectively of platinum in the electrolyte. The cathodic current efficiency remains constant over the whole range of current densities at 87%.

At current densities higher than 600 A m^{-2}, the current/voltage relationship is linear, indicating the total predominance of the IR_{cell} term in Equation 7. The observed cell voltages vary between 1.29 V at 0.6 kA m^{-2} and 1.61 V at 4.0 kA m^{-2}. As foreseen, the addition of a platinum salt to the electrolyte leads to a cell voltage decrease of approximately 80 to 100 mV. The cell voltage is important as it determines the energy consumption of the cell. The energy consumption at 2 kA m^{-2} and 50° C is equal to 0.55 kWh kg^{-1} of Br_2. The decrease in cell voltage due to the addition of platinum corresponds to a decrease in energy consumption of about 5 to 10%.

4.2. *Influence of temperature*

Temperatures above ambient are frequently used in industrial electrolysis, because of the beneficial effects on the kinetics of all steps in an electrode process. The exchange current density for both anodic and cathodic reactions is increased, diminishing thereby the overvoltages g_a and g_c in Equation 7. On the other hand, an increase in T leads to an increase in the electrolyte conductivity and hence to a decrease in the cell resistance, R_{cell}. The cell voltage was examined at three different current densities (2, 3, and 4 kA m^{-2}) and at three different temperatures (46, 50 and 56° C), in normal operating conditions. Figure 4 summarizes these results. An increase of 10° C in temperature leads to 80 to 100 mV decrease in the cell voltage, i.e. a decrease of 5% in energy consumption.

4.3. *The electrochemical efficiency*

4.3.1. Anodic and cathodic current efficiency measurements. This experiment was carried out as described in Section 3.2, at a current density of 2 kA m^{-2} and a flow rate of 260 kg h^{-1}. For 20 min, 100 A were passed through the cell, which gave rise to a theoretical formation of 0.62 mol of H_2 and Br_2. At the end of the experiment, 10.9 litres of hydrogen was obtained (0.49 mol) corresponding to a cathodic current efficiency of 78%. The bromine concentration in the electrolyte at the end of the experiment was 23 mmol kg^{-1}. This corresponds, for 20 kg of electrolyte, to an anodic current efficiency of 74%. A good correspondence was therefore observed between anodic and cathodic current efficiencies.

4.3.2. Influence of the inlet bromine concentration. This experiment was carried out at different values of the current density (between 1.0 and 4.0 kA m^{-2}) and at an electrolyte flow rate of 230 kg h^{-1}. The results for 1.0, 1.5 and 2.0 kA m^{-2} are presented in Fig. 5. The negative effect of the inlet bromine concentration C_{in} on the current efficiency is clearly shown. At 1 kA m^{-2} for instance, it drops from 83% to 32% when C_{in} is increased from 6.4 to 41.6 mmol l^{-1}. Figure 5 gives the

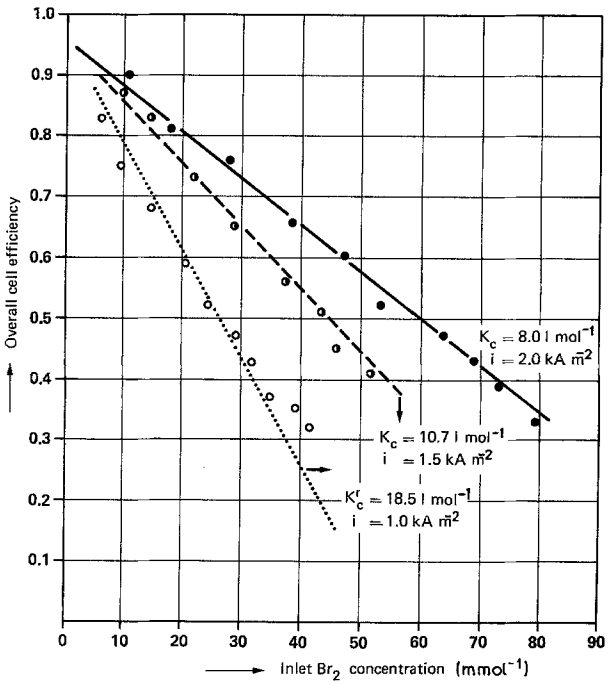

Fig. 5. The effect of bromine concentration on current efficiency.

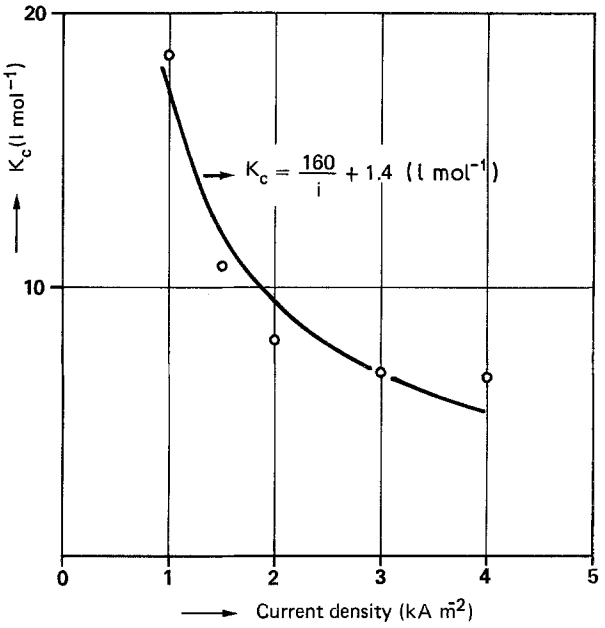

Fig. 6. The back reaction rate constant as a function of current density.

dependence of the overall cell efficiency as a function of the inlet bromine concentration, showing different curves for each current density.

Each experimental condition can be represented by a linear relationship, which indicates that the assumption that the cathodic back reaction is first order in bromine concentration is justified. According to the practice described earlier (Equations 15 and 16), a best fit value for K_c was calculated for each experimental condition. The calculated values are given in Table 1 and Fig. 6. It follows that the reaction rate constant is strongly dependent on the current density. This dependency can be expressed by:

$$K_c = 16.0/i + 1.4 \quad (l\,mol^{-1}) \qquad (17)$$

The rate equation for the cathodic back reaction can then be obtained by a rearrangement of Equations 5 and 12 and is

$$w_b = (0.298 + 0.026i)C \quad (mol\,m^{-2}\,h^{-1}) \qquad (18)$$

Equation 18 was developed on the basis of the phenomena occuring in a laboratory-size DEM cell. It provides an adequate description of the local processes occurring in the cell. Therefore it also offers a suitable basis for the prediction of the back reaction rates, and thus current efficiencies, in a larger size cell, provided this cell consists of the same electrode material and is working at the same temperature. Most probably, the numerical values of the rate constant K_c depend on the cell temperature and the cathode material. Extrapolation of Equation 18 to other cell conditions is thus very questionable, and should be avoided.

Table 1. The effect of current density on the cathodic back reaction rate constant

Current density ($kA\,m^{-2}$)	K_c ($l\,mol^{-1}$)
1.0	18.5
1.5	10.7
2.0	8.0
3.0	6.9
4.0	6.7

4.3.3. Influence of the electrolyte flow rate. The cathodic current efficiency was measured in normal operating conditions, at $2\,kA\,m^{-2}$, at different values of the electrolyte flow rate. These results are summarized in Table 2. The influence of the flow rate on the current efficiency is clearly shown: the efficiency increases with increasing electrolyte flow rate from 85 to 94%. These results are to be expected. Indeed, an increase in G, the electrolyte flow rate, leads to a decrease in the bromine concentration inside the cell, and thus the rate of the cathodic back reaction must also decrease. The direct consequence is a higher current efficiency.

The simple reaction model developed earlier can be applied to predict the effect of an increase of the electrolyte flow rate. The calculated values are given in the last column of Table 2. It can be concluded that the predicted values and the experimental data correlate satisfactorily.

5. Long duration experiments

5.1. *Cell performance*

The DEM cell was tested in a number of long duration experiments, where especially cell performance and stability were of importance. This work had to yield a design basis for a larger scale DEM cell to be built in the Ispra Mark 13A pilot plant in Sarroch. This cell is designed to produce 170 kg of bromine as a 1 wt% solution at a current density of $2.0\,kA\,m^{-2}$. The electrode surface area is $32\,m^2$ and the cell is of the bipolar,

Table 2. The influence of the flow rate on the electrochemical efficiency

$T(°C)$	*Flow* ($kg\,h^{-1}$)	*Velocity* ($cm\,s^{-1}$)	*Br_2 inlet concentration* ($mmol\,l^{-1}$)	*Efficiency* (%)	*Calculated (Eqn 16) efficiency*
50	162	3.60	8.1	85	86.8
50	212	4.74	6.1	88	89.7
50	232	5.19	4.1	92	92.0
50	244	5.46	2.2	94	93.8

filter press type. The laboratory type DEM cell was operated in combination with the Ispra Mark 13A bench scale plant for more than 1500 h under the conditions given below:

Flue gas flow rate	$10–12\,m^3\,h^{-1}$
SO_2 inlet	3500 ppm
SO_2 outlet	100–200 ppm
Electrolyte composition	
H_2SO_4	14–16 wt%
HBr	14–16 wt%
Electrolyte flow rate	$200\,l\,h^{-1}$
Cell temperature	43° C
Current density	$2.0\,kA\,m^{-2}$
Cell voltage	1.40–1.45 V
Current efficiency	90%

The results of this long-time experiment were very satisfactory. The cell was operating in a stable manner and no signs of wear were observed. The experiments were also used to get an insight into the corrosion phenomena encountered in the cell, and these are discussed below.

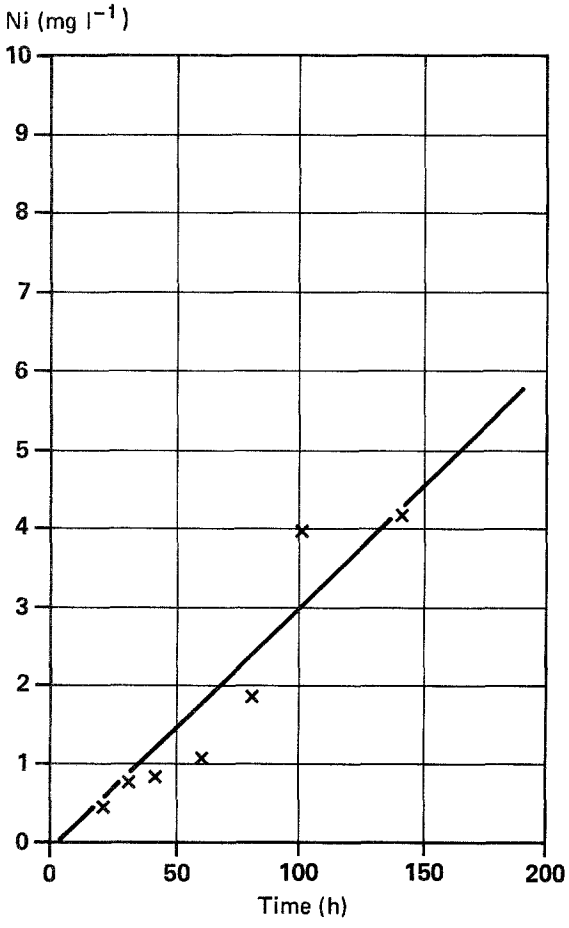

Fig. 7. Evolution of the nickel content of the electrolyte with time.

5.2. *The cathode*

The cathode material is Hastelloy 276 C. The chemical composition of this alloy is: Ni 60%, Cr 15%, Mo 16%, Fe 5%, W 4%, Mn 1% and traces of Si, V, P and S. The main constituent is thus nickel. Therefore, the change in the nickel content of the electrolyte gives an indication of the rate of corrosion of the cathode. This rate was determined by taking samples of the reactor liquid at regular time intervals and analysing the nickel content of the electrolyte. Figure 7 represents the change in the nickel content of the electrolyte. There is an almost linear increase of the nickel content with time. After 140 h of operation, the Ni concentration is $4.2\,mg\,l^{-1}$. For an electrolyte hold-up of 20 kg and a cathode surface of $0.05\,m^2$ this is equivalent to a corrosion rate of about $10\,mg\,m^{-2}\,h^{-1}$. This value can be extrapolated and it can be concluded that the corrosion rate will be approximately 0.01 mm per year. This is an acceptable figure.

5.3. *The anode*

The accelerated life tests carried out in the laboratory were carried out as described in Section 2.6. The cell was operated at ambient temperature at a current of 4A, equivalent to an anodic current density of $4\,kA\,m^{-2}$. A typical electrolyte (15 wt% HBr–20 wt% H_2SO_4) was used. After about 24 h the rate of anodic bromine evolution was equivalent to the rate of reduction of the bromine at the large cathode. In this condition, the bromine concentration was $50\,g\,l^{-1}$. From time to time, the total bromine and bromide concentration was measured and a small amount of hydrobromic acid was added when necessary. The total electrolyte level was checked weekly and, when necessary, demineralized water was added.

Three types of anode coating were tested: ruthenium dioxide coated on titanium, ruthenium dioxide coated on stabilized titanium and platinum/iridium coated on titanium. The latter coating is more usually used for oxygen evolving anodes, but it was thought worthwhile to test it in this series. After periods of approximately 300, 1200 and 2000 h, the test anodes were removed and the coating thickness measured. A total of four nearly identical anodes of each type were supplied. Three of these were put into the test cell and

Table 3. Relative coating thickness measurements

	Electrode	*Start*	*After 290 h*	*After 1250 h*	*After 1950 h*
RuO_2 on titanium	I.1 (standard)	0.96 ± 0.1	1.02 ± 0.1	1.00 ± 0.1	1.03 ± 0.1
	I.2	0.99 ± 0.2	1.01 ± 0.2	1.02 ± 0.3	1.01 ± 0.2
	I.3	0.71 ± 0.2	0.71 ± 0.2	0.68 ± 0.2	0.74 ± 0.2
	I.4	0.90 ± 0.3	0.90 ± 0.2	0.96 ± 0.3	0.92 ± 0.2
RuO_2 on stabilised titanium	II.1 (standard)	1.02 ± 0.1	0.99 ± 0.1	1.03 ± 0.1	0.97 ± 0.1
	II.2	0.96 ± 0.1	1.01 ± 0.1	1.02 ± 0.05	1.00 ± 0.1
	II.3	0.90 ± 0.1	0.94 ± 0.1	0.90 ± 0.1	0.90 ± 0.1
	II.4	1.16 ± 0.1	1.08 ± 0.1	1.04 ± 0.1	1.12 ± 0.1
Pt/Ir on titanium	III.1 (standard)	1.00 ± 0.2	1.00 ± 0.2	0.99 ± 0.1	1.00 ± 0.2
	III.2	1.10 ± 0.2	1.05 ± 0.2	0.69 ± 0.2	0.74 ± 0.2
	III.3	1.09 ± 0.2	0.87 ± 0.1	0.82 ± 0.2	0.68 ± 0.2
	III.4	0.97 ± 0.1	0.81 ± 0.1	0.68 ± 0.2	0.65 ± 0.1

the fourth retained as a standard. Consequently, the first anode in each of the sets in the results (Table 3) was not used. This gives an independent check on the instrument. The mean of four measurements on each standard was taken as unity.

It can be seen that the two ruthenium dioxide coated anodes show no measurable wear during the time of the test. In contrast, the mixed oxide (platinum irridium) coating shows significant wear, the three results being much the same at about 40% coating loss in 2000 h. An optimistic estimate of the life of this anode is a little over six months. In contrast, the life of the ruthenium coated anodes cannot be estimated from this data.

The pilot plant anode coating was essentially the same as the two ruthenium dioxide coatings tested in the laboratory. A template was cut and placed over the electrode such that the same 36 regularly spaced areas were monitored on each occasion. No external standard was available, but at the time of each measurement, 12 areas on the outside edge of the electrode were monitored. These areas had not been in contact with the electrolyte and could serve as an internal standard.

The first thing to notice about the results (Table 4) is that the edge of the anode appears to have a thicker coating than the face. This is a real effect and almost certainly a result of the coating process. The results are essentially the same as those from the accelerated life tests and may be expressed in terms of grams of coating per surface area. Although nearly within the limits of error, the final measurement (1510 h) does suggest that some coating wear may have occured. Clearly a much longer trial is needed to be sure of this. However, if the observed wear rate is real, it would indicate an anode life in excess of three years. Finally, it must be said that the conditions in the pilot plant, with its higher temperature of operation, must be more severe than those in the laboratory test cell.

Table 4. Anode coating thickness measurements (pilot plant)

	Coating thickness ($g\,m^{-2}$)			
	Start	*680 h*	*830 h*	*1510 h*
Edge	16.0 ± 3.5	17.7 ± 3.5	16.3 ± 3.4	15.9 ± 3.3
Face	13.3 ± 3.0	13.9 ± 2.5	13.7 ± 3.0	12.8 ± 3.0

References

[1] D. Halstead, *The Chemical Engineer* **443** (1987) 13.
[2] J. Redman, *The Chemical Engineer* **453** (1988) 29.
[3] L. Himsl and P. Reichel, *VGB Kraftwerkstechnik* **68** (1988) 56.
[4] C. E. Jahnig and H. Shaw, *J. Air Poll. Control Ass.* **31** (1981) 421.
[5] K. Scott, T. Fannon and J. Winnick, *J. Electrochem. Soc.* **135** (1988) 573.
[6] D. van Velzen, H. Langenkamp and G. F. De Beni, 'Process for the removal of SO_2 from waste gases, producing hydrogen and sulphuric acid'; Eur. patent n° 0.016290.
[7] D. van Velzen and H. Langenkamp, 'Ispra Mark 13A, a new process for flue gas desulphurization', Achema Conference, Frankfurt (1988).
[8] P. J. Fiebelmann and G. H. Schütz, *Int. J. Hydrogen Energy* **5** (1980) 305.
[9] H. Fees, K. Köster and G. H. Schütz, *Int. J. Hydrogen Energy* **6** (1981) 377.
[10] D. Hughes, *The Chemical Engineer* **441** (1987) 17.
[11] D. Pletcher, in 'Industrial Electrochemistry' (edited by D. Pletcher), Chapman and Hall, London (1984) Chap. 3, pp. 88–113.
[12] A. J. Scarpellino and G. L. Fisher, *J. Electrochem. Soc.* **129** (1982) 515–522.
[13] S. Trasatti, *J. Electrochem. Soc.* **39** (1972) 163.
[14] M. Pourbaix, in 'Atlas of Electrochemical Equilibria in Aqueous Solutions', Pergamon Press, London (English edition) Chap. IV, Sect. 12.3, 330.